

# Particular Solutions of Singularly Perturbed Partial Differential Equations with Constant Coefficients in Rectangular Domains, Part II: Computational Aspects

Hsin-Yun Hu\*, Heng-Shuing Tsai†, Zi-Cai Li‡ and Song Wang§

January 13, 2005

## Abstract

This is a continued study on the solution of convection-diffusion equations with boundary layers. In our previous work, Part I, the solutions of the homogenous singularly perturbed differential equations with Dirichlet boundary conditions are expressed in a series of particular solutions have been proposed, based on the separation of variables. In this study we extend our previous results to the homogeneous equations with anisotropic diffusion coefficients, and to non-homogeneous equations. Moreover, we will discuss in detail computational aspects of the methods for three different models of fast convergence. Among them, the model with waterfalls solutions is especially interesting, because it presents an intrinsic nature of singular boundary layers. A new convergence analysis for a model of the non-homogeneous equation is also performed in this work. Numerical results for  $\epsilon = 10^{-7}$  will be presented for all models, where  $\epsilon$  denotes the singular perturbation parameter. The numerical solutions for  $\epsilon = 0.1$  are also illustrated to give a clear view of the solutions of the singularly perturbed partial differential equations. Finally, we propose a collocation Trefftz method using the particular solutions obtained in the work. Results from numerical experiments on the collocation Trefftz methods will be presented.

**Keywords:** Singularly perturbed equation, particular solutions, separation of variables, waterfalls solutions, collocation Trefftz method.

## 1 Introduction

Computational models play an important role in numerical solutions of partial differential equations (PDEs) because they provide not only solution behaviors (known or unknown),

---

\*Corresponding author: National Center for Theoretical Sciences Mathematics Division, National Tsing Hua University, Hsinchu, Taiwan 30043, E-mail: huhu@math.cts.nthu.edu.tw

†Department of Applied Mathematics, National Sun Yat-sen University, Kaohsiung, Taiwan 80424

‡Department of Applied Mathematics and Department of Computer Science and Engineering, National Sun Yat-sen University, Kaohsiung, Taiwan 80424

§School of Mathematics and Statistics, The University of Western Australia, Perth, WA 6009, Australia

but also benchmarks for testing numerical methods. For example, Motz's problem is an excellent model of pointwise singularity problems which has been used by many authors (see [4, 9]). Singularly perturbed partial differential equations cause more difficulties in computation than Motz's and other pointwise singularity problems, such as angular singularities, interface singularities and infinities (refer [4]). The main difficulty in the singularly perturbed PDEs is that the solution exhibits sharp boundary layers when the singularly perturbed parameter,  $\epsilon$ , approaches zero.

Our objectives of this work are to seek suitable computational models of singularly perturbed convection-diffusion equations with constant coefficients in special domains such as rectangles or sectors. This work is a sequential study of [5] to focus on computational aspects. Details of motivation for this study and the related references have been given in [5] and two recent textbooks [10, 11].

In this work we seek particular solutions in the form of Fourier series to singularly perturbed PDEs using separation of variables [3]. The unknown coefficients in the particular solutions are determined by forcing the solutions to satisfy the Dirichlet boundary conditions exactly. The series solutions with finite terms can be used as numerical models in practical computations. This is called a boundary method, or the Trefftz method in engineering terminology. The collocation Trefftz method, the Schwarz alternating method, and their combinations may be used to seek solutions of high accuracy. In this work we will report some numerical results by the collocation Trefftz method.

In previous work [5], the properties of convergence and error bounds are addressed, but only some preliminary numerical results are reported. In what follows we will continue to use the notation used in [5]. The current work provides the following new aspects.

1. For waterfalls solutions of Model  $I_M$ , the solutions with two thin boundary layers near boundaries are given in numerical results for  $\epsilon = 10^{-7}$ . Comparing with Model  $I$  in [5] with slow convergence, we here provide an innovative model with fast convergence. Such an improvement in convergence is important and essential to develop a benchmark of boundary layer problem. To distinguish Model  $I$  in [5], Model  $I_M$  is called a modification of Model  $I$  in this work.
2. For spikes solutions of Model  $II$ , the solutions with four needle-like towers are given in numerical results for  $\epsilon = 10^{-7}$ . In [5], the algorithms with two towers are given, but no numerical results were reported.
3. A new model, called Model  $III$ , is designed for the non-homogeneous singularly perturbed PDEs. Error analysis will be performed, and numerical solutions will also be reported.

This work is organized as follows. In the next section, we describe basic approaches to finding particular solutions, which consist of the methods with and without the corner zero conditions. In Section 3, we present the methods for non-homogeneous equations, and the homogeneous equations with anisotropic diffusion coefficients. In Sections 4–6, we explore three computational models with convergence analysis. In Section 7, the collocation Trefftz method is used to seek an approximate solution for a model. Some conclusions are summarized in the last section.

## 2 Basic Approaches

Consider singularly perturbed partial differential equations with the Dirichlet boundary condition of the form

$$\mathcal{L}w = -\epsilon \left( \frac{\partial^2 w}{\partial x^2} + \frac{\partial^2 w}{\partial y^2} \right) + \alpha \frac{\partial w}{\partial x} + \beta \frac{\partial w}{\partial y} + cw = f(x, y) \quad \text{in } S, \quad (2.1)$$

$$w = g(x, y) \quad \text{on } \Gamma, \quad (2.2)$$

where  $S$  is the square  $S = \{(x, y), 0 < x < \pi, 0 < y < \pi\}$  and  $\Gamma$  is its boundary. The parameters  $\epsilon, \alpha, \beta$  and  $c(\geq 0)$  are all constants, but  $\epsilon$  may be very small:  $0 < \epsilon \ll 1$ .

In this study, we assume without loss of generality,  $\alpha, \beta \geq 0$ . There then exists a boundary layer occurring near the boundary segments at  $x = \pi$  and  $y = \pi$ . Since all parameters  $\epsilon, \alpha, \beta$  and  $c$  are constants, we seek analytic solutions to (2.1)-(2.2) by means of the separation of variables.

We decompose (2.1)-(2.2) into two problems,  $w = u + v$ , where  $u$  and  $v$  satisfy

$$\mathcal{L}u = 0 \quad \text{in } S, \quad u|_{\Gamma} = g(x, y), \quad (2.3)$$

and

$$\mathcal{L}v = f(x, y) \quad \text{in } S, \quad v|_{\Gamma} = 0, \quad (2.4)$$

respectively. We will first find the explicit solutions to (2.3) in Sections 2.1 and 2.2, and then those to (2.4) in Section 3.2.

### 2.1 Partial Solutions

For (2.3), let the Dirichlet boundary conditions along four edges of  $S$  be given by

$$\begin{aligned} u(x, 0) = g(x, 0) &=: g_1(x), & u(x, \pi) = g(x, \pi) &=: g_2(x), \\ u(0, y) = g(0, y) &=: g_3(y), & u(\pi, y) = g(\pi, y) &=: g_4(y), \end{aligned}$$

where the function  $g$  is continuous at the four corners so that the following corner continuity conditions hold:

$$g_1(0) = g_3(0), \quad g_1(\pi) = g_4(0), \quad g_3(\pi) = g_2(0), \quad g_2(\pi) = g_4(\pi).$$

Suppose that the boundary conditions at the four corners are zero,

$$g_i(0) = g_i(\pi) = 0, \quad i = 1, 2, 3, 4. \quad (2.5)$$

In this work we refer (2.5) to as the *corner zero conditions*. Now we split the problem (2.3) again into four sub-problems,  $u = \sum_{i=1}^4 u^{(i)}$ , where  $u^{(i)}$  satisfy

$$\begin{aligned} \mathcal{L}u^{(i)} &= 0, \quad \text{in } S, \\ u^{(i)}\Big|_{\Gamma_i} &= g_i, \quad u^{(i)}\Big|_{\Gamma \setminus \Gamma_i} = 0, \end{aligned} \quad (2.6)$$

where  $\Gamma = \cup_{i=1}^4 \Gamma_i$ . Denote

$$t_k = \left\{ k^2 + \frac{\alpha^2 + \beta^2 + 4\epsilon c}{4\epsilon^2} \right\}^{\frac{1}{2}}. \quad (2.7)$$

From the separation of variables, we obtain from [5] the following solutions satisfying (2.5),

$$\begin{aligned} u^{(1)} &= \exp\left(\frac{-\alpha(\pi - x) + \beta y}{2\epsilon}\right) \sum_{k=1}^{\infty} b_k \sinh(t_k(\pi - y)) \sin kx, \\ u^{(2)} &= \exp\left(\frac{-\alpha(\pi - x) + \beta y}{2\epsilon}\right) \sum_{k=1}^{\infty} a_k \sinh(t_k y) \sin kx, \end{aligned}$$

where the coefficients are defined by

$$a_k = \frac{2}{\pi} \frac{1}{\sinh(t_k \pi)} \int_0^{\pi} g_2(x) \exp\left(\frac{\alpha(\pi - x) - \beta \pi}{2\epsilon}\right) \sin kx dx, \quad (2.8)$$

$$b_k = \frac{2}{\pi} \frac{1}{\sinh(t_k \pi)} \int_0^{\pi} g_1(x) \exp\left(\frac{\alpha(\pi - x)}{2\epsilon}\right) \sin kx dx. \quad (2.9)$$

Also for  $u^{(3)}$  and  $u^{(4)}$ , we have

$$\begin{aligned} u^{(3)} &= \exp\left(\frac{\alpha x - \beta(\pi - y)}{2\epsilon}\right) \sum_{k=1}^{\infty} d_k \sinh(t_k(\pi - x)) \sin ky, \\ u^{(4)} &= \exp\left(\frac{\alpha x - \beta(\pi - y)}{2\epsilon}\right) \sum_{k=1}^{\infty} c_k \sinh(t_k x) \sin ky, \end{aligned}$$

where the coefficients are given by (see [5])

$$c_k = \frac{2}{\pi} \frac{1}{\sinh(t_k \pi)} \int_0^{\pi} g_4(y) \exp\left(\frac{-\alpha \pi + \beta(\pi - y)}{2\epsilon}\right) \sin ky dy, \quad (2.10)$$

$$d_k = \frac{2}{\pi} \frac{1}{\sinh(t_k \pi)} \int_0^{\pi} g_3(y) \exp\left(\frac{\beta(\pi - y)}{2\epsilon}\right) \sin ky dy. \quad (2.11)$$

In summary, we have the solution to (2.6) satisfying the corner zero conditions (2.5) as shown below.

$$\begin{aligned}
u &= \sum_{i=1}^4 u^{(i)} \\
&= \exp\left(\frac{-\alpha(\pi-x) + \beta y}{2\epsilon}\right) \sum_{k=1}^{\infty} \{a_k \sinh(t_k y) \sin kx + b_k \sinh(t_k(\pi-y)) \sin kx\} \\
&\quad + \exp\left(\frac{\alpha x - \beta(\pi-y)}{2\epsilon}\right) \sum_{k=1}^{\infty} \{c_k \sinh(t_k x) \sin ky + d_k \sinh(t_k(\pi-x)) \sin ky\},
\end{aligned}$$

where the coefficients  $a_k$ ,  $b_k$ ,  $c_k$  and  $d_k$  are given in (2.8), (2.9), (2.10) and (2.11), respectively.

## 2.2 The case that the corner zero conditions are not satisfied

Let  $\bar{u}$  be a transition function satisfying

$$\mathcal{L}\bar{u} = 0, \quad \text{in } S, \quad (2.12)$$

$$\bar{u}(0,0) = g(0,0), \quad \bar{u}(\pi,0) = g(\pi,0),$$

$$\bar{u}(0,\pi) = g(0,\pi), \quad \bar{u}(\pi,\pi) = g(\pi,\pi). \quad (2.13)$$

Hence the difference  $(u - \bar{u})$  satisfies (2.3) and the *corner zero conditions* (2.5). In this work we consider a different particular solution from that in [5] derived in [6]:

$$\begin{aligned}
\bar{u}(x,y) &= a_0 \sinh(t_\alpha x) \exp\left(-\frac{\alpha(\pi-x)}{2\epsilon}\right) + b_0 \sinh(t_\beta y) \exp\left(-\frac{\beta(\pi-y)}{2\epsilon}\right) \\
&\quad + c_0 \sinh(s_\alpha x) \sinh(s_\beta y) \exp\left(-\frac{\alpha(\pi-x) + \beta(\pi-y)}{2\epsilon}\right) \\
&=: v_1(x) + v_2(y) + v_3(x,y),
\end{aligned} \quad (2.14)$$

where

$$t_\alpha = \left\{ \frac{\alpha^2 + 4\epsilon c}{4\epsilon^2} \right\}^{\frac{1}{2}}, \quad s_\alpha = \left\{ \frac{\alpha^2 + 2\epsilon c}{4\epsilon^2} \right\}^{\frac{1}{2}}, \quad (2.15)$$

$$t_\beta = \left\{ \frac{\beta^2 + 4\epsilon c}{4\epsilon^2} \right\}^{\frac{1}{2}}, \quad s_\beta = \left\{ \frac{\beta^2 + 2\epsilon c}{4\epsilon^2} \right\}^{\frac{1}{2}}, \quad (2.16)$$

and the coefficients in (2.14) are determined to satisfy the boundary conditions (2.13). Moreover, the explicit solutions to (2.3) are given by

$$u(x,y) = \bar{u}(x,y)$$

$$\begin{aligned}
& + \exp\left(\frac{-\alpha(\pi - x) + \beta y}{2\epsilon}\right) \sum_{k=1}^{\infty} \{a_k \sinh(t_k y) \sin kx + b_k \sinh(t_k(\pi - y)) \sin kx\} \\
& + \exp\left(\frac{\alpha x - \beta(\pi - y)}{2\epsilon}\right) \sum_{k=1}^{\infty} \{c_k \sinh(t_k x) \sin ky + d_k \sinh(t_k(\pi - x)) \sin ky\}.
\end{aligned}$$

**Remark 2.1** In the previous work [5], we derived a similar particular solution, denoted as Model I, which is computationally very expensive when  $\epsilon$  is small. Model I proposed in [5] has a slow convergence rate. In [6], we improve this model and propose a new particular solution (2.14) to obtain a better model with fast convergence rate. For the details of this discussion we defer to [6].

### 3 Other problems

In this section we extend the approaches in previous section to the homogeneous equations with anisotropic diffusion coefficients, and to the non-homogeneous equations. In this discussion we will omit most of the proofs and concentrate on the results, as the proof are very similar to those in [5] and [6].

#### 3.1 Anisotropic Diffusion Coefficients

Consider

$$\begin{aligned}
-\epsilon_1 \frac{\partial^2 u}{\partial x^2} - \epsilon_2 \frac{\partial^2 u}{\partial y^2} + \alpha \frac{\partial u}{\partial x} + \beta \frac{\partial u}{\partial y} + cu &= 0 \quad \text{in } S, \\
u &= g(x, y) \quad \text{on } \Gamma,
\end{aligned} \tag{3.1}$$

where  $\epsilon_1$  and  $\epsilon_2$  are two small positive numbers. When  $\epsilon_1 = \epsilon_2$ , (3.1) leads to (2.3). By following the approaches in Section 2, we derive the particular solutions to (3.1) below.

Denote

$$\begin{aligned}
t_k^{(1)} &= \left\{ \frac{1}{\epsilon_2} \left( \epsilon_1 k^2 + \frac{\alpha^2}{4\epsilon_1} + \frac{\beta^2}{4\epsilon_2} + c \right) \right\}^{\frac{1}{2}}, \\
t_k^{(2)} &= \left\{ \frac{1}{\epsilon_1} \left( \epsilon_2 k^2 + \frac{\alpha^2}{4\epsilon_1} + \frac{\beta^2}{4\epsilon_2} + c \right) \right\}^{\frac{1}{2}}.
\end{aligned}$$

The explicit solutions to (3.1) can be found as

$$\begin{aligned}
u(x, y) &= \bar{u}(x, y) \\
& + \exp\left(-\frac{\alpha(\pi - x)}{2\epsilon_1} + \frac{\beta y}{2\epsilon_2}\right) \sum_{k=1}^{\infty} \{\bar{a}_k \sinh(t_k^{(1)} y) \sin kx + \bar{b}_k \sinh(t_k^{(1)}(\pi - y)) \sin kx\} \\
& + \exp\left(\frac{\alpha x}{2\epsilon_1} - \frac{\beta(\pi - y)}{2\epsilon_2}\right) \sum_{k=1}^{\infty} \{\bar{c}_k \sinh(t_k^{(2)} x) \sin ky + \bar{d}_k \sinh(t_k^{(2)}(\pi - x)) \sin ky\}.
\end{aligned}$$

The coefficients  $\bar{a}_k, \bar{b}_k, \bar{c}_k$  and  $\bar{d}_k$  can be obtained, and the particular solution  $\bar{u}(x, y)$  is given by

$$\begin{aligned} \bar{u}(x, y) &= \bar{a}_0 \sinh(\bar{t}_\alpha x) \exp\left(-\frac{\alpha(\pi - x)}{2\epsilon_1}\right) + \bar{b}_0 \sinh(\bar{t}_\beta y) \exp\left(-\frac{\beta(\pi - y)}{2\epsilon_2}\right) \\ &+ \bar{c}_0 \sinh(\bar{s}_\alpha x) \sinh(\bar{s}_\beta y) \exp\left(-\frac{\alpha(\pi - x)}{2\epsilon_1} - \frac{\beta(\pi - y)}{2\epsilon_2}\right), \end{aligned} \quad (3.2)$$

where

$$\begin{aligned} \bar{t}_\alpha &= \left\{ \frac{\alpha^2 + 4\epsilon_1 c}{4\epsilon_1^2} \right\}^{\frac{1}{2}}, \quad \bar{s}_\alpha = \left\{ \frac{\alpha^2 + 2\epsilon_1 c}{4\epsilon_1^2} \right\}^{\frac{1}{2}}, \\ \bar{t}_\beta &= \left\{ \frac{\beta^2 + 4\epsilon_2 c}{4\epsilon_2^2} \right\}^{\frac{1}{2}}, \quad \bar{s}_\beta = \left\{ \frac{\beta^2 + 2\epsilon_2 c}{4\epsilon_2^2} \right\}^{\frac{1}{2}}. \end{aligned} \quad (3.3)$$

Note that (3.2) is slightly different from (2.14).

### 3.2 Non-homogeneous equations

In this subsection, we consider the non-homogeneous equations (2.4) on  $S^* = \{(x, y), 0 < x < 2\pi, 0 < y < 2\pi\}$ . Let

$$v = \exp\left(\frac{\alpha x + \beta y}{2\epsilon}\right) \hat{w},$$

we obtain from (2.4)

$$-\epsilon \left( \frac{\partial^2}{\partial x^2} + \frac{\partial^2}{\partial y^2} \right) \hat{w} + \left( \frac{\alpha^2 + \beta^2}{4\epsilon} + c \right) \hat{w} = \bar{f}(x, y) \quad \text{in } S^*, \quad (3.4)$$

$$\hat{w} = 0 \quad \text{on } \Gamma^*, \quad (3.5)$$

where  $\Gamma^*$  is the boundary of  $S^*$ , and

$$\bar{f}(x, y) = \exp\left(-\frac{\alpha x + \beta y}{2\epsilon}\right) f(x, y).$$

By some algebraic manipulations, the particular solutions  $\bar{w}$  of (3.4) are obtained as

$$\begin{aligned} \bar{w} &= a_0^* + \sum_{k=1}^{\infty} (a_k^* \sin kx + b_k^* \sin ky) \\ &+ \sum_{k, \ell=1}^{\infty} (a_{k, \ell} \cos kx \cos \ell y + b_{k, \ell} \cos kx \sin \ell y + c_{k, \ell} \sin kx \cos \ell y + d_{k, \ell} \sin kx \sin \ell y), \end{aligned}$$

where the coefficients are given by

$$\begin{aligned}
a_0^* &= \frac{1}{4\pi^2 p_{0,0}} \int_0^{2\pi} \int_0^{2\pi} \bar{f}(x, y) dx dy, \\
a_k^* &= \frac{1}{2\pi^2 p_{k,0}} \int_0^{2\pi} \int_0^{2\pi} \bar{f}(x, y) \sin kx dx dy, \\
b_k^* &= \frac{1}{2\pi^2 p_{k,0}} \int_0^{2\pi} \int_0^{2\pi} \bar{f}(x, y) \sin ky dx dy, \\
a_{k,\ell} &= \frac{1}{\pi^2 p_{k,\ell}} \int_0^{2\pi} \int_0^{2\pi} \bar{f}(x, y) \cos kx \cos \ell y dx dy, \\
b_{k,\ell} &= \frac{1}{\pi^2 p_{k,\ell}} \int_0^{2\pi} \int_0^{2\pi} \bar{f}(x, y) \cos kx \sin \ell y dx dy, \\
c_{k,\ell} &= \frac{1}{\pi^2 p_{k,\ell}} \int_0^{2\pi} \int_0^{2\pi} \bar{f}(x, y) \sin kx \cos \ell y dx dy, \\
d_{k,\ell} &= \frac{1}{\pi^2 p_{k,\ell}} \int_0^{2\pi} \int_0^{2\pi} \bar{f}(x, y) \sin kx \sin \ell y dx dy,
\end{aligned} \tag{3.6}$$

and

$$p_{k,\ell} = \epsilon(k^2 + \ell^2) + \frac{\alpha^2 + \beta^2}{4\epsilon} + c.$$

Hence, let  $\tilde{w} = \hat{w} - \bar{w}$ , we have from (3.4) and (3.5)

$$-\epsilon \left( \frac{\partial^2}{\partial x^2} + \frac{\partial^2}{\partial y^2} \right) \tilde{w} + \left( \frac{\alpha^2 + \beta^2}{4\epsilon} + c \right) \tilde{w} = 0 \quad \text{in } S^*, \tag{3.7}$$

$$\tilde{w} = -\bar{w} \quad \text{on } \Gamma^*. \tag{3.8}$$

For the homogeneous equation (3.7) with the Dirichlet boundary condition (3.8), we may obtain the exact solutions from Section 2. If  $f(x, y)$  is an elementary function, it is possible to evaluate exactly the integrals on the right-hand sides in (3.6) and thus to derive explicit expressions for  $a_0^*$ ,  $a_k^*$ ,  $b_k^*$ ,  $a_{k,\ell}$ , etc. (cf. [1, 2]).

Let us consider a special case that

$$f(x, y) = \exp\left(\frac{\alpha x + \beta y}{2\epsilon}\right) s(x)s(y), \tag{3.9}$$

where

$$s(x) = \frac{\pi^4 x}{90} - \frac{\pi^2 x^3}{36} + \frac{\pi x^4}{48} - \frac{x^5}{240} = \sum_{k=1}^{\infty} \frac{\sin kx}{k^5}. \tag{3.10}$$

The equality on the right hand of the above is given in [2]. We obtain the solution of (2.4)

$$v = \exp\left(\frac{\alpha x + \beta y}{2\epsilon}\right) \sum_{k,\ell=1}^{\infty} a_{k,\ell} \sin kx \sin \ell y, \tag{3.11}$$

where the coefficients are given by

$$\begin{aligned}
a_{k,\ell} &= \frac{1}{\pi^2 p_{k,\ell}} \int_0^{2\pi} \int_0^{2\pi} f(x, y) \exp\left(-\frac{\alpha x + \beta y}{2\epsilon}\right) \sin kx \sin \ell y dx dy \\
&= \frac{1}{p_{k,\ell}} \left( \frac{1}{\pi} \int_0^{2\pi} s(x) \sin kx dx \right) \left( \frac{1}{\pi} \int_0^{2\pi} s(y) \sin \ell y dy \right) \\
&= \frac{1}{k^5 \ell^5 p_{k,\ell}}.
\end{aligned} \tag{3.12}$$

In summary, we have found the following explicit solutions to (2.1)-(2.2),

$$\begin{aligned}
w &= \bar{u} + \exp\left(\frac{\alpha x + \beta y}{2\epsilon}\right) \sum_{k,\ell=1}^{\infty} a_{k,\ell} \sin kx \sin \ell y \\
&+ \exp\left(\frac{-\alpha(2\pi - x) + \beta y}{2\epsilon}\right) \sum_{k=1}^{\infty} \{a_k \sinh(t_k y) \sin kx + b_k \sinh(t_k(2\pi - y)) \sin kx\} \\
&+ \exp\left(\frac{\alpha x - \beta(2\pi - y)}{2\epsilon}\right) \sum_{k=1}^{\infty} \{c_k \sinh(t_k x) \sin ky + d_k \sinh(t_k(2\pi - x)) \sin ky\},
\end{aligned}$$

where the coefficients  $a_{k,\ell}$  are given in (3.12),  $a_k, b_k, c_k$  and  $d_k$  in (2.8)–(2.11), respectively, and the solution  $\bar{u}$  in (2.14).

## 4 Model $I_M$ with waterfalls solutions

In [5], we propose a computational model with waterfalls solutions, called Model  $I$ . However, the convergence rate of its solutions is slow. A modified model with fast convergence rate is designed, and called Model  $I_M$  in this study. In this section we will report some computational aspects for such a modified model.

The Model  $I_M$  with two boundary layers is designed on the domain  $S \cup \partial S = [0, \pi]^2$ . We choose the corner conditions as follows

$$u(0, 0) = 0, \quad u(\pi, 0) = u(0, \pi) = u(\pi, \pi) = 1, \tag{4.1}$$

and consider the following particular solution corresponding to (2.14)

$$\begin{aligned}
\bar{u}(x, y) &= a_0 \sinh(t_\alpha x) \exp\left(-\frac{\alpha(\pi - x)}{2\epsilon}\right) + b_0 \sinh(t_\beta y) \exp\left(-\frac{\beta(\pi - y)}{2\epsilon}\right) \\
&+ c_0 \sinh(s_\alpha x) \sinh(s_\beta y) \exp\left(-\frac{\alpha(\pi - x) + \beta(\pi - y)}{2\epsilon}\right),
\end{aligned}$$

where  $t_\alpha, t_\beta, s_\alpha$  and  $s_\beta$  are given in (2.15) and (2.16), respectively. Applying (4.1) to  $\bar{u}$  defined above gives

$$a_0 = \frac{1}{\sinh(t_\alpha \pi)}, \quad b_0 = \frac{1}{\sinh(t_\beta \pi)}, \quad c_0 = \frac{-1}{\sinh(s_\alpha \pi) \sinh(s_\beta \pi)}.$$

Hence, we have the particular solutions

$$\begin{aligned} \bar{u}(x, y) &= \frac{\sinh(t_\alpha x)}{\sinh(t_\alpha \pi)} \exp\left(-\frac{\alpha(\pi - x)}{2\epsilon}\right) + \frac{\sinh(t_\beta y)}{\sinh(t_\beta \pi)} \exp\left(-\frac{\beta(\pi - y)}{2\epsilon}\right) \\ &- \frac{\sinh(s_\alpha x) \sinh(s_\beta y)}{\sinh(s_\alpha \pi) \sinh(s_\beta \pi)} \exp\left(-\frac{\alpha(\pi - x) + \beta(\pi - y)}{2\epsilon}\right). \end{aligned} \quad (4.2)$$

#### 4.1 The general case with two regular boundary layers

We design the waterfalls model on  $S$  determined by the equation

$$\mathcal{L}u = -\epsilon \left( \frac{\partial^2 u}{\partial x^2} + \frac{\partial^2 u}{\partial y^2} \right) + \alpha \frac{\partial u}{\partial x} + \beta \frac{\partial u}{\partial y} + cu = 0,$$

and the boundary conditions

$$\begin{aligned} u(x, \pi) &= u(\pi, y) = 1, \\ u(x, 0) &= \frac{\sinh(t_\alpha x)}{\sinh(t_\alpha \pi)} \exp\left(-\frac{\alpha(\pi - x)}{2\epsilon}\right) = \bar{u}(x, 0) =: g_1(x), \\ u(0, y) &= \frac{\sinh(t_\beta y)}{\sinh(t_\beta \pi)} \exp\left(-\frac{\beta(\pi - y)}{2\epsilon}\right) = \bar{u}(0, y) =: g_3(y). \end{aligned}$$

The solutions are then found by

$$\begin{aligned} u(x, y) &= \bar{u}(x, y) \\ &+ \exp\left(\frac{-\alpha(\pi - x) + \beta y}{2\epsilon}\right) \sum_{k=1}^{\infty} a_k \frac{\sinh(t_k y)}{\sinh(t_k \pi)} \sin kx \\ &+ \exp\left(\frac{\alpha x - \beta(\pi - y)}{2\epsilon}\right) \sum_{k=1}^{\infty} c_k \frac{\sinh(t_k x)}{\sinh(t_k \pi)} \sin ky, \end{aligned} \quad (4.3)$$

where  $\bar{u}(x, y)$  is given in (4.2),  $t_k$  is given in (2.7), and the coefficients are

$$\begin{aligned} a_k &= \frac{2}{\pi} \int_0^\pi (1 - \bar{u}(x, \pi)) \exp\left(\frac{\alpha(\pi - x) - \beta\pi}{2\epsilon}\right) \sin kx \, dx, \\ c_k &= \frac{2}{\pi} \int_0^\pi (1 - \bar{u}(\pi, y)) \exp\left(\frac{-\alpha\pi + \beta(\pi - y)}{2\epsilon}\right) \sin ky \, dy. \end{aligned}$$

Using the integration formula

$$\int_0^\pi \sinh(tx) \sin kx \, dx = \sinh(t\pi) \frac{k(-1)^{k+1}}{k^2 + t^2},$$

the coefficients  $a_k$  and  $c_k$  can be expressed as

$$\begin{aligned} a_k &= \frac{2}{\pi} \frac{k(-1)^k (s_\alpha^2 - t_\alpha^2)}{(k^2 + s_\alpha^2)(k^2 + t_\alpha^2)} \exp\left(-\frac{\beta\pi}{2\epsilon}\right), \\ c_k &= \frac{2}{\pi} \frac{k(-1)^k (s_\beta^2 - t_\beta^2)}{(k^2 + s_\beta^2)(k^2 + t_\beta^2)} \exp\left(-\frac{\alpha\pi}{2\epsilon}\right). \end{aligned}$$

Furthermore, we rewrite the solutions (4.3) as

$$\begin{aligned} u(x, y) &= \bar{u}(x, y) + \exp\left(\frac{-\alpha(\pi - x) - \beta(\pi - y)}{2\epsilon}\right) \\ &\times \sum_{k=1}^{\infty} \left\{ \tilde{a}_k \frac{\sinh(t_k y)}{\sinh(t_k \pi)} \sin kx + \tilde{c}_k \frac{\sinh(t_k x)}{\sinh(t_k \pi)} \sin ky \right\}, \end{aligned} \quad (4.4)$$

where the coefficients are

$$\begin{aligned} \tilde{a}_k &= \frac{c}{\pi\epsilon} \frac{k(-1)^{k+1}}{\left(k^2 + \frac{\alpha^2 + 2\epsilon c}{4\epsilon^2}\right) \left(k^2 + \frac{\alpha^2 + 4\epsilon c}{4\epsilon^2}\right)}, \\ \tilde{c}_k &= \frac{c}{\pi\epsilon} \frac{k(-1)^{k+1}}{\left(k^2 + \frac{\beta^2 + 2\epsilon c}{4\epsilon^2}\right) \left(k^2 + \frac{\beta^2 + 4\epsilon c}{4\epsilon^2}\right)}. \end{aligned}$$

In this case the solutions consist of two regular layers of width  $O(\epsilon)$  near the boundary segments at  $x = \pi$  and  $y = \pi$ . It follows that the solution derivatives  $u_x$  and  $u_y$  are both of order  $O(\frac{1}{\epsilon})$ . We shall discuss the widths of the layers in more details in Section 4.3.

Choosing the first  $N$  terms, we have the following approximation to the solutions

$$\begin{aligned} u_N(x, y) &= \bar{u}(x, y) + \exp\left(\frac{-\alpha(\pi - x) - \beta(\pi - y)}{2\epsilon}\right) \\ &\times \sum_{k=1}^N \left\{ \tilde{a}_k \frac{\sinh(t_k y)}{\sinh(t_k \pi)} \sin kx + \tilde{c}_k \frac{\sinh(t_k x)}{\sinh(t_k \pi)} \sin ky \right\}. \end{aligned} \quad (4.5)$$

For the error in  $u_N$  we cite the following theorem from [6].

**Theorem 4.1** *Let  $\epsilon \in (0, 1]$ . For Model  $I_M$  with  $\alpha \geq \beta > 0$  and  $c > 0$ , there exist the error bounds,*

$$|u - u_N| \leq \frac{c\epsilon}{2\pi} \left\{ \frac{1}{\epsilon^2 N^2 + \frac{\alpha^2 + 2\epsilon c}{4}} + \frac{1}{\epsilon^2 N^2 + \frac{\beta^2 + 2\epsilon c}{4}} \right\} \quad (4.6)$$

$$\begin{aligned} &\times \exp\left(-\frac{\alpha(\pi - x) + \beta(\pi - y)}{2\epsilon}\right), \\ | \epsilon(u_y - (u_N)_y) | &\leq \frac{3}{1 - \exp(-(\frac{\alpha}{2} + \sqrt{c})\pi)} \frac{c}{\pi} \left\{ \frac{1}{N} + \frac{\epsilon(\frac{\beta}{\sqrt{2}} + \sqrt{c})}{\epsilon^2 N^2 + \frac{\beta^2 + 2\epsilon c}{4}} \right\} \\ &\times \exp\left(-\frac{\alpha(\pi - x) + \beta(\pi - y)}{2\epsilon}\right). \end{aligned} \quad (4.7)$$

Computationally, the errors are required to satisfy

$$|u - u_N| \leq \delta, \quad |\epsilon(u_y - (u_N)_y)| \leq \delta, \quad (4.8)$$

where  $\delta > 0$  is a chosen tolerance, then we have the following corollary.

**Corollary 4.1** *Let the assumptions in Theorem 4.1 hold. To achieve (4.8), we may choose*

$$N = \left\{ O\left(\frac{1}{\sqrt{\delta\epsilon}}\right) + O\left(\frac{1}{\delta}\right) \right\} \times \exp\left(-\frac{\alpha(\pi - x) + \beta(\pi - y)}{2\epsilon}\right) \quad (4.9)$$

for  $\epsilon \geq 10^{-4}$ ,

$$N = O\left(\frac{1}{\delta}\right) \times \exp\left(-\frac{\alpha(\pi - x) + \beta(\pi - y)}{2\epsilon}\right) \quad (4.10)$$

for  $\epsilon \leq 10^{-4}$ .

**Remark 4.1** *It is surprising that the term number  $N$  needed is small when  $\epsilon$  approaches zero. In fact, to satisfy  $|u - u_N| \leq \delta$ , we may even choose  $N = 0$ , i.e.,  $u_0 = \bar{u}(x, y)$  in (4.5). Such a remarkable result can be seen from (4.6),*

$$\max_{\bar{S}} |u - u_0| \leq \frac{c\epsilon}{2\pi} \left( \frac{4}{\alpha^2} + \frac{4}{\beta^2} \right) \leq \frac{4c\epsilon}{\pi\beta^2} \leq \delta,$$

when  $\epsilon \leq \frac{\pi\beta^2}{4c}\delta$ . Next, to satisfy  $|\epsilon(u_y - (u_N)_y)| \leq \delta$ , which reflects the relative error of  $(u_N)_y$ , we obtain (4.10) from (4.7) immediately. Note that for the location  $(x, y)$  not near the corner  $(\pi, \pi)$ , the term number  $N$  may also be chosen much smaller. In Table 1, we choose only  $N = 1$  for  $\epsilon = 10^{-7}$ . Comparing with the original Model I in [5], we have, indeed, made a great improvement on convergence rates for the models with waterfalls solutions.

Let  $\alpha = \beta = c = 1$ , and the solutions of Model  $I_M$  have two regular boundary layers along  $x = \pi$  and  $y = \pi$ . First, we choose  $N = 130$  for  $\epsilon = 0.1$  and obtain from (4.5) the solutions and derivatives along  $y = \pi - \mu\epsilon$  where  $\mu = 1 - 5$ . Since the solutions in this case are symmetric in  $x$  and  $y$ , we omit the solutions and derivatives along  $x = \pi - \mu\epsilon$ . The level curves of solutions and derivatives for  $\epsilon = 0.1$  near  $y = \pi$  are plotted in Figure 1. In order to give a clear view of the solutions behavior, we draw in Figure 2 the profile of solution  $u$ . Next, choose  $N = 1$  for  $\epsilon = 10^{-7}$ , the values of solutions and derivatives along  $y = \pi - \epsilon$  are listed in Table 1. From Figure 1 and Table 1, it is seen that the normal derivatives of order  $O(\frac{1}{\epsilon})$  near the boundary segments at  $x = \pi$  and  $y = \pi$ .

## 4.2 Problems with a parabolic boundary layer

Following the above discussion, we consider the case with  $\beta = 0$ . The particular solution  $\bar{u}(x, y)$  in (4.2) becomes

$$\begin{aligned} \bar{u}(x, y) &= \frac{\sinh(t_\alpha x)}{\sinh(t_\alpha \pi)} \exp\left(-\frac{\alpha(\pi - x)}{2\epsilon}\right) + \frac{\sinh(t_\gamma y)}{\sinh(t_\gamma \pi)} \\ &- \frac{\sinh(s_\alpha x) \sinh(s_\gamma y)}{\sinh(s_\alpha \pi) \sinh(s_\gamma \pi)} \exp\left(-\frac{\alpha(\pi - x)}{2\epsilon}\right), \end{aligned} \quad (4.11)$$

where

$$t_\gamma = \sqrt{\frac{c}{\epsilon}}, \quad s_\gamma = \sqrt{\frac{c}{2\epsilon}}. \quad (4.12)$$

In this case the solution consists of a parabolic layer of width  $O(\sqrt{\epsilon})$  near the segment at  $y = \pi$ . It follows that the derivative  $u_x$  is of order  $\frac{1}{\epsilon}$ , whereas the derivative  $u_y$  is of order  $\frac{1}{\sqrt{\epsilon}}$ . Eq. (4.3), together with (4.11), defines the particular solution to the problem defined in Section 4.1 with  $\beta = 0$ . In practice, we only choose a finite number of terms in the series in (4.3) to form an approximation to the series solution. If we denote this approximation by  $u_N$ , where  $N$  denotes the number of terms, then the truncation error of this approximation is given in the following theorem.

**Theorem 4.2** *Let  $\epsilon \in (0, 1]$ . For Model  $I_M$  with  $\alpha > 0, \beta = 0$  and  $c > 0$ , there exist the error bounds,*

$$|u - u_N| \leq \frac{c\epsilon}{2\pi} \left\{ \frac{1}{\epsilon^2 N^2 + \frac{\alpha^2 + 2\epsilon c}{4}} + \frac{1}{\epsilon^2 N^2 + \frac{\epsilon c}{2}} \right\} \times \exp\left(-\frac{\alpha(\pi - x)}{2\epsilon}\right), \quad (4.13)$$

$$\begin{aligned} |\sqrt{\epsilon}(u_y - (u_N)_y)| &\leq \frac{3}{1 - \exp(-\sqrt{c}\pi)} \frac{c}{\pi} \left\{ \frac{1}{N\sqrt{\epsilon}} + \frac{\sqrt{c}}{\epsilon\sqrt{\epsilon}N^2 + \frac{c}{2}\sqrt{\epsilon}} \right\} \\ &\times \exp\left(-\frac{\alpha(\pi - x)}{2\epsilon}\right). \end{aligned} \quad (4.14)$$

If we request the above errors to satisfy

$$|u - u_N| \leq \delta, \quad |\sqrt{\epsilon}(u_y - (u_N)_y)| \leq \delta, \quad (4.15)$$

and then  $N$  is determined by the following corollary.

**Corollary 4.2** *Let all the assumptions in Theorem 4.2 hold. To achieve (4.15) we may choose*

$$N = \left\{ O\left(\frac{1}{\epsilon^{\frac{3}{4}}\sqrt{\delta}}\right) + O\left(\frac{1}{\sqrt{\epsilon}\delta}\right) \right\} \times \exp\left(-\frac{\alpha(\pi - x)}{2\epsilon}\right).$$

**Remark 4.2** From Corollary 4.2 we see that  $N$  is of order  $O(\epsilon^{-\frac{3}{4}})$  when  $\delta$  is fixed,  $\epsilon \rightarrow 0$  and  $x$  is sufficiently close to  $\pi$ . However, when  $(x, y)$  is not near the corner  $(\pi, \pi)$ , the term number  $N$  can be chosen much smaller because of the exponential term in the above estimate. Comparing with the previous case with regular layers, we need much more terms in this case.

Some numerical experiments have been performed for the case that  $\alpha = c = 1$  and  $\beta = 0$ . The computed solution for  $N = 180$  and  $\epsilon = 0.1$  is depicted in Figure 3. Comparing with Figure 2, the width of the parabolic layer near the boundary segment at  $y = \pi$  is wider than that of the regular layer. For the case  $\epsilon = 10^{-7}$ , we choose  $N = 1$  except for the derivatives at  $x = \pi$  and  $y = \pi - \sqrt{\epsilon}$  for which we choose  $N \approx O(10^4)$ . The computed values of the solution and derivatives along  $y = \pi - \sqrt{\epsilon}$  are listed in Table 2. Although the solutions in this case are non-symmetric in  $x$  and  $y$ , we still omit the solutions along  $x$ -direction because we are only interested in the behavior of the parabolic layer of the problem. From Table 2 we see that the values of the normal derivative  $u_y$  are of roughly  $O(\frac{1}{\sqrt{\epsilon}})$ . Hence the termination large near the segment at  $y = \pi$ , being  $O(\frac{1}{\sqrt{\epsilon}})$ . Hence the termination condition in (4.15) also reflects somehow the relative errors of  $(u_N)_y$ .

### 4.3 The widths of layers for Model $I_M$

In this subsection we discuss the widths of both regular and parabolic layers. The width of a boundary layer is an important feature because the solution varies rapidly within this region. These widths can be used for dividing the solution domain into two either disjoint or overlapped subdomains so that the solution in one of the subregions is sufficiently smooth. We may use two different methods in the two different subdomains to solve such a problem, i.e., the combined or alternating methods (cf., for example, [12]). We now provide a definition concerning the boundary width of a solution and derivatives to Model  $I_M$ . It will be useful in practical computations.

For simplicity, we only consider the layer near boundary  $y = \pi$  and first focus on a subdomain, denoted as  $\hat{S}$ , of  $S$  far from the corner  $(\pi, \pi)$ . We define the widths,  $\omega_0$  and  $\omega_1$ , of a regular layer as

$$\begin{aligned} u(x, y) &\geq 10^{-r}, \quad \text{when } y \geq \pi - \omega_0, \\ u_y(x, y) &\geq 10^{-r}, \quad \text{when } y \geq \pi - \omega_1, \end{aligned} \tag{4.16}$$

and the widths,  $\bar{\omega}_0$  and  $\bar{\omega}_1$ , of a parabolic layer as

$$\begin{aligned} u(x, y) &\geq 10^{-r}, \quad \text{when } y \geq \pi - \bar{\omega}_0, \\ u_y(x, y) &\geq 10^{-r}, \quad \text{when } y \geq \pi - \bar{\omega}_1, \end{aligned} \tag{4.17}$$

where  $r$  is a positive integer greater than 1. We look for the widths in the form

$$\begin{aligned} \omega_i &= d_i \epsilon, \quad i = 0, 1, \\ \bar{\omega}_i &= \bar{d}_i \sqrt{\epsilon}, \quad i = 0, 1. \end{aligned}$$

The coefficients  $d_i$  and  $\bar{d}_i$  can then be derived by (4.16) and (4.17) as follows

$$d_0 = \frac{r}{\beta} \ln 10, \quad d_1 = d_0 + \frac{1}{\beta} \ln \frac{\beta}{\epsilon}, \quad (4.18)$$

$$\bar{d}_0 = \frac{r}{\sqrt{c}} \ln 10, \quad \bar{d}_1 = \bar{d}_0 + \frac{1}{\sqrt{c}} \ln \frac{\sqrt{c}}{\sqrt{\epsilon}}. \quad (4.19)$$

**Remark 4.3** For all values of  $\epsilon$  the lower bound  $10^{-r}$  is selected in order to make both  $d_0$  and  $\bar{d}_0$  constants. In fact, we may follow the idea in [10] to define the widths of a regular boundary layer as

$$\begin{aligned} u(x, y) &\geq \epsilon, \quad \text{when } y \geq \pi - \omega_0, \\ u_y(x, y) &\geq C, \quad \text{when } y \geq \pi - \omega_1, \end{aligned}$$

and the widths of a parabolic one as

$$\begin{aligned} u(x, y) &\geq \sqrt{\epsilon}, \quad \text{when } y \geq \pi - \bar{\omega}_0, \\ u_y(x, y) &\geq C, \quad \text{when } y \geq \pi - \bar{\omega}_1, \end{aligned}$$

where  $C$  is a constant (eg unity). The constants  $d_0$  and  $\bar{d}_0$  are then dependent of  $\ln \frac{1}{\epsilon}$  and  $\ln \frac{1}{\sqrt{\epsilon}}$ , respectively.

Now, let us briefly derive the estimates in (4.18). Consider the following one-dimensional model

$$\begin{aligned} -\epsilon u''(y) + \beta u'(y) + cu(y) &= 0, \quad 0 < y < \pi, \\ u(0) &= 0, \quad u(\pi) = 1. \end{aligned}$$

We then have the following approximate solution and its derivative

$$\begin{aligned} u(y) &= \frac{\sinh(t_\beta y)}{\sinh(t_\beta \pi)} \exp\left(-\frac{\beta(\pi - y)}{2\epsilon}\right) \approx \exp\left(-\frac{\beta}{\epsilon}(\pi - y)\right), \\ u'(y) &\approx \frac{\beta}{\epsilon} \exp\left(-\frac{\beta}{\epsilon}(\pi - y)\right). \end{aligned}$$

Using (4.16), we have

$$\begin{aligned} u(\pi - d_0\epsilon) &\approx \exp(-\beta d_0) \geq 10^{-r}, \\ u'(\pi - d_1\epsilon) &\approx \frac{\beta}{\epsilon} \exp(-\beta d_1) \geq 10^{-r}. \end{aligned}$$

Taking the logarithm on both sides, we obtain the desired formulas (4.18) after some manipulations.

We now derive the estimates in (4.19). Consider the following one-dimensional model of the form

$$\begin{aligned} -\epsilon u''(y) + cu(y) &= 0, \quad 0 < y < \pi, \\ u(0) &= 0, \quad u(\pi) = 1. \end{aligned}$$

The approximate solution and its derivative are respectively given by

$$\begin{aligned} u(y) &= \frac{\sinh(\sqrt{\frac{c}{\epsilon}}y)}{\sinh(\sqrt{\frac{c}{\epsilon}}\pi)} \approx \exp\left(-\sqrt{\frac{c}{\epsilon}}(\pi - y)\right), \\ u'(y) &\approx \sqrt{\frac{c}{\epsilon}} \exp\left(-\sqrt{\frac{c}{\epsilon}}(\pi - y)\right). \end{aligned}$$

From (4.17), we have

$$\begin{aligned} u(\pi - \bar{d}_0\sqrt{\epsilon}) &\approx \exp(-\sqrt{c\bar{d}_0}) \geq 10^{-r}, \\ u'(\pi - \bar{d}_1\sqrt{\epsilon}) &\approx \sqrt{\frac{c}{\epsilon}} \exp(-\sqrt{c\bar{d}_1}) \geq 10^{-r}. \end{aligned}$$

Solving these inequalities gives (4.19).

**Remark 4.4** *Although the estimates in (4.18) and (4.19) are derived from the one-dimensional problems, they are still valid for the subdomain  $\hat{S}$  far from the corner  $(\pi, \pi)$ . We see that there exists a regular layer of width  $O(\epsilon)$  near the boundary segment at  $y = \pi$  in Figure 2, whereas there exists a parabolic layer of width  $O(\sqrt{\epsilon})$  near the boundary segment at  $y = \pi$  in Figure 3.*

Finally, let us discuss the widths near the corner  $(\pi, \pi)$ . We know that there exists a superposition of two layers along both  $y = \pi$  and  $x = \pi$ . Here, we consider the widths of the regular layer for  $\alpha = \beta > 0$ . Define the widths,  $\omega_0^*$  and  $\omega_1^*$ , near  $(\pi, \pi)$  for the regular layers by

$$\omega_i^* = d_i^* \epsilon, \quad i = 0, 1.$$

We have the following approximations directly from (4.4)

$$\begin{aligned} u(\pi - \omega_0^*, \pi - \omega_0^*) &\approx 2 \exp(-\alpha d_0^*) \geq 10^{-r}, \\ u_n(\pi - \omega_1^*, \pi - \omega_1^*) &\approx \frac{\alpha}{\epsilon} \exp(-\alpha d_1^*) \geq 10^{-r}, \end{aligned}$$

where  $u_n = u_x = u_y$ . After some manipulation, we obtain

$$d_0^* = \frac{r}{\alpha} \ln 10 + \frac{1}{\alpha} \ln 2, \quad d_1^* = \frac{r}{\alpha} \ln 10 + \frac{1}{\alpha} \ln \frac{\alpha}{\epsilon}. \quad (4.20)$$

Comparing this with (4.18), we see that  $d_0^*$  is larger than  $d_0$  by the quantity  $\frac{1}{\alpha} \ln 2$ , whereas the  $d_1^*$  is equal to  $d_1$ . The derivation of the case of the parabolic layer can be proceed in a same way.

In what follows we investigate the transition from a regular layer of width  $O(\epsilon)$  to a parabolic layer of width  $O(\sqrt{\epsilon})$ . We take the case with  $\alpha, c > 0$ , and  $\beta = 0$  as an example.

For simplicity, we merely focus on the particular solution  $\bar{u}(x, y)$  in (4.11)

$$\begin{aligned} \bar{u}(x, y) \approx & \exp\left(-\left(t_\alpha + \frac{\alpha}{2\epsilon}\right)(\pi - x)\right) + \exp(-t_\gamma(\pi - y)) \\ & - \exp\left(-\left(s_\alpha + \frac{\alpha}{2\epsilon}\right)(\pi - x) - s_\gamma(\pi - y)\right), \end{aligned} \quad (4.21)$$

where  $t_\alpha$  and  $s_\alpha$  are given in (2.15) and  $t_\gamma$  and  $s_\gamma$  given in (4.12). Choosing  $\alpha = O(1)$ , we then have the following relations

$$t_\alpha = O\left(\frac{1}{\epsilon}\right), \quad s_\alpha = O\left(\frac{1}{\epsilon}\right), \quad \frac{\alpha}{2\epsilon} = O\left(\frac{1}{\epsilon}\right).$$

It follows that there exists a regular layer of  $O(\epsilon)$  near the boundary segment at  $x = \pi$ . If we choose  $\alpha = O(\sqrt{\epsilon})$ , then the relations become

$$t_\alpha = O\left(\frac{1}{\sqrt{\epsilon}}\right), \quad s_\alpha = O\left(\frac{1}{\sqrt{\epsilon}}\right), \quad \frac{\alpha}{2\epsilon} = O\left(\frac{1}{\sqrt{\epsilon}}\right).$$

At this time the boundary layer near  $x = \pi$  becomes a parabolic layer of  $O(\sqrt{\epsilon})$ . Next, we choose  $\alpha = O(\epsilon^p)$ ,  $0 < p < \frac{1}{2}$ , then obtain

$$t_\alpha = O\left(\frac{1}{\sqrt{\epsilon}}\right) + O\left(\frac{1}{\epsilon^{1-p}}\right) = O\left(\frac{1}{\epsilon^{1-p}}\right), \quad s_\alpha = O\left(\frac{1}{\epsilon^{1-p}}\right), \quad \frac{\alpha}{2\epsilon} = O\left(\frac{1}{\epsilon^{1-p}}\right).$$

A transitional layer between the regular and the parabolic boundary layers occurs with the width of  $O(\epsilon^{1-p})$ .

We summarize above results as a corollary.

**Corollary 4.3** *Let  $\beta = 0, c = 1, \epsilon \rightarrow 0$  and*

$$\alpha = O(\epsilon^p), \quad 0 \leq p < \infty. \quad (4.22)$$

*For the solutions of Model  $I_M$ , the parabolic layer is located at  $y = \pi$ , but the type of boundary layer near the boundary segment at  $x = \pi$  is dependent of the power  $p$  in (4.22):*

- (1) *when  $p = 0$ , a regular boundary layer of width  $O(\epsilon)$ .*
- (2) *when  $p \geq \frac{1}{2}$ , a parabolic boundary layer of width  $O(\sqrt{\epsilon})$ .*
- (3) *when  $p \in (0, \frac{1}{2})$ , the transitional layers of width  $O(\epsilon^{1-p})$ .*

## 5 Model II with spikes solutions

In this section we derive another computational model with explicit solutions containing only a few expansion terms. Let us consider the problem  $\mathcal{L}u = 0$  on  $S = (0, \pi)^2$  with the following Dirichlet conditions (see [5])

$$\begin{aligned} u(x, 0) &= \gamma \exp(p \cos x) \sin(p \sin x) \exp\left(-\frac{\alpha(\pi - x)}{2\epsilon}\right) =: g_1(x), \\ u(x, \pi) &= \gamma \exp(p \cos x) \sin(p \sin x) \exp\left(-\frac{\alpha(\pi - x)}{2\epsilon}\right) =: g_2(x), \\ u(0, y) &= \gamma \exp(p \cos y) \sin(p \sin y) \exp\left(-\frac{\beta(\pi - y)}{2\epsilon}\right) =: g_3(y), \\ u(\pi, y) &= \gamma \exp(p \cos y) \sin(p \sin y) \exp\left(-\frac{\beta(\pi - y)}{2\epsilon}\right) =: g_4(y), \end{aligned} \quad (5.1)$$

where  $p^2 \leq 1$ , and  $\gamma$  is a parameter to adjust the solutions to be  $O(1)$ . This model is referred to as Model II, and the solution is given by

$$u(x, y) = \sum_{k=1}^{\infty} \{a_k \phi_k(x, y) + b_k \psi_k(x, y) + a_k^* \phi_k^*(x, y) + b_k^* \psi_k^*(x, y)\}, \quad (5.2)$$

where

$$\begin{aligned} \phi_k(x, y) &= \exp\left(\frac{-\alpha(\pi - x) + \beta y}{2\epsilon}\right) \frac{\sinh(t_k(\pi - y))}{\sinh(t_k \pi)} \sin kx, \\ \psi_k(x, y) &= \exp\left(\frac{\alpha x - \beta(\pi - y)}{2\epsilon}\right) \frac{\sinh(t_k(\pi - x))}{\sinh(t_k \pi)} \sin ky, \\ \phi_k^*(x, y) &= \exp\left(\frac{-\alpha(\pi - x) - \beta(\pi - y)}{2\epsilon}\right) \frac{\sinh(t_k y)}{\sinh(t_k \pi)} \sin kx, \\ \psi_k^*(x, y) &= \exp\left(\frac{-\alpha(\pi - x) - \beta(\pi - y)}{2\epsilon}\right) \frac{\sinh(t_k x)}{\sinh(t_k \pi)} \sin ky. \end{aligned} \quad (5.3)$$

Based on the formula in [2],

$$\sum_{k=1}^{\infty} \frac{p^k \sin kt}{k!} = \exp(p \cos t) \sin(p \sin t), \quad p \leq 1,$$

we derive from the orthogonality of trigonometric functions

$$a_k = b_k = a_k^* = b_k^* = \gamma \frac{p^k}{k!}, \quad (5.4)$$

where  $\gamma$  is given as

$$\gamma = \frac{\alpha}{2\epsilon p} \exp(p + \alpha), \quad \text{or} \quad \gamma = \frac{\beta}{2\epsilon p} \exp(p + \beta). \quad (5.5)$$

In this model there are four spikes in the solution (5.2), while the model given in [5] similar to this has two spikes.

For a positive integer  $N$ , we define the following approximation to the solution in (5.2)

$$u_N = \sum_{k=1}^N \{a_k \phi_k(x, y) + b_k \psi_k(x, y) + a_k^* \phi_k^*(x, y) + b_k^* \psi_k^*(x, y)\}, \quad (5.6)$$

Then, we have the following error bounds (see [5]).

**Theorem 5.1** *For the solutions of Model II with  $p \leq 1$ , there exists the error bound,*

$$\max_{\bar{S}} |u - u_N| \leq 4\gamma \frac{p^{N+1}}{N!N}. \quad (5.7)$$

Moreover, suppose  $\beta \leq \alpha$ , and  $N \leq \frac{1}{\epsilon}$  for  $\epsilon \ll 1$ , there exist the bounds,

$$\begin{aligned} \max_{\bar{S}} |\epsilon(u_x - (u_N)_x)| &\leq C_1 \gamma \frac{p^{N+1}}{N!N}, \\ \max_{\bar{S}} |\epsilon(u_y - (u_N)_y)| &\leq C_1 \gamma \frac{p^{N+1}}{N!N}, \end{aligned} \quad (5.8)$$

where  $C_1 = 6(1 + \alpha)$ .

Note that these estimates show very fast convergence in  $N$ . Take (5.8) for example. Supposing that we require the maximal error of the derivative is less than  $\delta > 0$ , we have

$$|\epsilon(u_x - (u_N)_x)| \leq C_1 \gamma \frac{p^{N+1}}{N!N} \leq \delta. \quad (5.9)$$

When  $\delta = 5 \times 10^{-5}$ , and  $\epsilon \ll 1$ , the value of  $N$  needed is from 10 to 15 for  $\epsilon = 0.1 - 10^{-7}$ .

Numerical experiments have been performed for this model. In the numerical computation, we used (5.6) with  $p = 1$  and  $\alpha = \beta = c = 1$ . Various values of  $\epsilon$  and  $N$  have been used in the numerical experiments. The pointwise values of the numerical solutions and their derivatives for  $\epsilon = 10^{-7}$  and  $N = 15$  along  $y = \pi - \epsilon$  are listed in Table 3. The profile of solutions for  $\epsilon = 0.1$  is plotted in Figure 4. The solutions have four towers at  $(\pi - 2\epsilon, 0)$ ,  $(\pi - 2\epsilon, \pi)$ ,  $(0, \pi - 2\epsilon)$  and  $(\pi, \pi - 2\epsilon)$  with the heights being close to one. It is observed numerically that the convergence of the solutions (5.6) is very fast for all values of  $\epsilon$  ranging from  $10^{-7}$  to 0.1.

## 6 Model III of non-homogeneous equations

In this section we also pursue a new model with fast convergent rates, of which the solutions satisfy the non-homogeneous equation  $\mathcal{L}u = f$  in  $S^* = (0, 2\pi)^2$  with the homogeneous

Dirichlet boundary conditions. This model is called Model *III*. The function  $f$  is chosen to be

$$f(x, y) = \exp\left(\frac{-\alpha(2\pi - x) - \beta(2\pi - y)}{2\epsilon}\right) s(x)s(y), \quad (6.1)$$

where  $s(x)$  is given in (3.10). The solution to  $\mathcal{L}u = f$  is given by

$$\begin{aligned} u(x, y) &= \nu^2 \exp\left(\frac{-\alpha(2\pi - x) - \beta(2\pi - y)}{2\epsilon}\right) \sum_{k,\ell=1}^{\infty} a_{k,\ell} \sin kx \sin \ell y \\ &= \exp\left(\frac{-\alpha(2\pi - x) - \beta(2\pi - y)}{2\epsilon}\right) \sum_{k,\ell=1}^{\infty} \bar{a}_{k,\ell} \sin kx \sin \ell y, \end{aligned} \quad (6.2)$$

where  $\nu$  is a parameter used to control the magnitude of the solution so that it is of order  $O(1)$  and the coefficients are given by

$$\bar{a}_{k,\ell} = \nu^2 a_{k,\ell} = \frac{\nu^2}{k^5 \ell^5 p_{k,\ell}}. \quad (6.3)$$

Let  $k \leq \frac{1}{\epsilon}$  and  $\ell \leq \frac{1}{\epsilon}$ , we then have  $k^2 + \ell^2 \leq \frac{2}{\epsilon^2}$ , and

$$p_{k,\ell} = \epsilon(k^2 + \ell^2) + \frac{\alpha^2 + \beta^2}{4\epsilon} + c \approx O\left(\frac{1}{\epsilon}\right). \quad (6.4)$$

Hence

$$|\bar{a}_{k,\ell}| \leq C \frac{\epsilon \nu^2}{k^5 \ell^5}. \quad (6.5)$$

Let us determine the parameter  $\nu$ . Consider the function

$$F(x) = \nu \exp\left(-\frac{\alpha(2\pi - x)}{2\epsilon}\right) s(x).$$

Then  $f(x, y) = F(x)F(y)$ . Since the maximal value of  $F(x)$  is located near  $x = 2\pi$ . From the Taylor formula, we have

$$s(x) = s(2\pi) + s'(2\pi)(x - 2\pi) + O((x - 2\pi)^2) \approx \frac{\pi^4}{90}(x - 2\pi),$$

where  $s(2\pi) = 0$  and  $s'(2\pi) = \frac{\pi^4}{90}$ . When  $x \rightarrow 2\pi$ , we define a new function

$$\hat{F}(x) = \nu \frac{\pi^4}{90}(x - 2\pi) \exp\left(-\frac{\alpha(2\pi - x)}{2\epsilon}\right),$$

and then  $F(x) \approx \hat{F}(x)$ . The maximum of  $\hat{F}(x)$  is located at  $x = \bar{x}$  to satisfy

$$0 = \hat{F}'(\bar{x}) = \nu \frac{\pi^4}{90} \exp\left(-\frac{\alpha(2\pi - \bar{x})}{2\epsilon}\right) \left(1 + \frac{\alpha(\bar{x} - 2\pi)}{2\epsilon}\right).$$

Solving this gives  $\bar{x} = 2\pi - \frac{2\epsilon}{\alpha}$ . Thus, we obtain

$$|\hat{F}(\bar{x})| = \nu \frac{\pi^4}{90} (\bar{x} - 2\pi) \exp\left(-\frac{\alpha(2\pi - \bar{x})}{2\epsilon}\right) = \nu \frac{\pi^4}{45e} \frac{\epsilon}{\alpha}.$$

To achieve  $|\hat{F}(\bar{x})| \approx O(1)$ , we may choose

$$\nu = \frac{45e}{\pi^4} \frac{\alpha}{\epsilon} = \nu_0 \frac{\alpha}{\epsilon}, \quad (6.6)$$

where

$$\nu_0 = \frac{45e}{\pi^4} \approx 1.2558.$$

From (6.5) and (6.6), we obtain

$$|\bar{a}_{k,\ell}| \leq C \frac{1}{\epsilon k^5 \ell^5}. \quad (6.7)$$

Let  $u_{M,N}$  be the partial sum of the solution (6.2) given by

$$u_{M,N} = \exp\left(\frac{-\alpha(2\pi - x) - \beta(2\pi - y)}{2\epsilon}\right) \sum_{k=1}^M \sum_{\ell=1}^N \bar{a}_{k,\ell} \sin kx \sin \ell y. \quad (6.8)$$

We have the following theorem.

**Theorem 6.1** *For the solutions of Model III, assume that  $M$  and  $N$  are positive integers satisfying  $M, N \leq \frac{1}{\epsilon}$ , there exist the error bounds,*

$$|u - u_{M,N}| \leq C \left( \frac{1}{\epsilon M^4} + \frac{1}{\epsilon N^4} \right) \exp\left(\frac{\alpha(x - 2\pi) + \beta(y - 2\pi)}{2\epsilon}\right), \quad (6.9)$$

$$|\epsilon(u_x - (u_{M,N})_x)| \leq C \left( \frac{1}{\epsilon M^4} + \frac{1}{\epsilon N^4} + \frac{1}{M^3} \right) \exp\left(\frac{\alpha(x - 2\pi) + \beta(y - 2\pi)}{2\epsilon}\right), \quad (6.10)$$

$$|\epsilon(u_y - (u_{M,N})_y)| \leq C \left( \frac{1}{\epsilon M^4} + \frac{1}{\epsilon N^4} + \frac{1}{N^3} \right) \exp\left(\frac{\alpha(x - 2\pi) + \beta(y - 2\pi)}{2\epsilon}\right), \quad (6.11)$$

where  $C$  is a positive constant, independent of  $\epsilon, M$  and  $N$ .

**Proof :** We have from (6.2), (6.7) and (6.8)

$$\begin{aligned} |u - u_{M,N}| &\leq \exp\left(\frac{\alpha(x-2\pi) + \beta(y-2\pi)}{2\epsilon}\right) \left( \sum_{k=M+1}^{\infty} \sum_{\ell=1}^{\infty} + \sum_{k=1}^{\infty} \sum_{\ell=N+1}^{\infty} \right) |\bar{a}_{k,\ell}| \\ &\leq C \exp\left(\frac{\alpha(x-2\pi) + \beta(y-2\pi)}{2\epsilon}\right) \left( \sum_{k=M+1}^{\infty} \sum_{\ell=1}^{\infty} + \sum_{k=1}^{\infty} \sum_{\ell=N+1}^{\infty} \right) \frac{1}{\epsilon k^5 \ell^5}. \end{aligned}$$

For the second last term in the above, we have

$$\begin{aligned} \sum_{k=M+1}^{\infty} \sum_{\ell=1}^{\infty} \frac{1}{\epsilon k^5 \ell^5} &= \frac{1}{\epsilon} \left( \sum_{k=M+1}^{\infty} \frac{1}{k^5} \right) \left( \sum_{\ell=1}^{\infty} \frac{1}{\ell^5} \right) \\ &\leq \frac{1}{\epsilon} \left( \int_M^{\infty} \frac{dt}{t^5} \right) \left( 1 + \int_1^{\infty} \frac{dt}{t^5} \right) = \frac{1}{\epsilon} \frac{1}{4M^4} \left( 1 + \frac{1}{4} \right) = \frac{5}{16} \frac{1}{\epsilon M^4}. \end{aligned}$$

Similarly, we have

$$\sum_{k=1}^{\infty} \sum_{\ell=N+1}^{\infty} \frac{1}{\epsilon k^5 \ell^5} \leq \frac{5}{16} \frac{1}{\epsilon N^4}.$$

Combining the above three inequalities gives the first result (6.9).

Next, we have

$$\begin{aligned} |u_x - (u_{M,N})_x| &\leq \frac{\alpha}{2\epsilon} |u - u_{M,N}| \\ &+ \exp\left(\frac{\alpha(x-2\pi) + \beta(y-2\pi)}{2\epsilon}\right) \left( \sum_{k=M+1}^{\infty} \sum_{\ell=1}^{\infty} + \sum_{k=1}^{\infty} \sum_{\ell=N+1}^{\infty} \right) k |\bar{a}_{k,\ell}|. \end{aligned} \tag{6.12}$$

The last two sums of the above can be estimated by

$$\begin{aligned} \sum_{k=M+1}^{\infty} \sum_{\ell=1}^{\infty} k |\bar{a}_{k,\ell}| &= \frac{C}{\epsilon} \left( \sum_{k=M+1}^{\infty} \frac{1}{k^4} \right) \left( \sum_{\ell=1}^{\infty} \frac{1}{\ell^5} \right) \leq \frac{C}{\epsilon M^3}, \\ \sum_{k=1}^{\infty} \sum_{\ell=N+1}^{\infty} k |\bar{a}_{k,\ell}| &= \frac{C}{\epsilon} \left( \sum_{k=1}^{\infty} \frac{1}{k^4} \right) \left( \sum_{\ell=N+1}^{\infty} \frac{1}{\ell^5} \right) \leq \frac{C}{\epsilon N^4}. \end{aligned}$$

Using these two inequalities, we have from (6.9)

$$|\epsilon(u_x - (u_{M,N})_x)| \leq C \left( \frac{1}{\epsilon M^4} + \frac{1}{\epsilon N^4} + \frac{1}{M^3} + \frac{1}{N^4} \right) \exp\left(\frac{\alpha(x-2\pi) + \beta(y-2\pi)}{2\epsilon}\right).$$

This is the second desired result (6.10). The proof for (6.11) is similar to that of the above and thus is omitted here. This completes the proof of Theorem 6.1. ■

In practical computations, we may request the truncation errors to satisfy

$$|u - u_{M,N}| \leq \delta, \quad |\epsilon(u_x - (u_{M,N})_x)| \leq \delta, \quad |\epsilon(u_y - (u_{M,N})_y)| \leq \delta. \quad (6.13)$$

The estimates of  $M$  and  $N$  for (6.13) to hold are given in the following corollary.

**Corollary 6.1** *Let the assumptions in Theorem 6.1 hold. To achieve (6.13), we may choose*

$$M, N = O\left(\frac{1}{(\delta\epsilon)^{\frac{1}{4}}}\right) + O\left(\frac{1}{\delta^{\frac{1}{3}}}\right).$$

We can see from Corollary 6.1 that  $M$  and  $N$  are of order  $\epsilon^{-\frac{1}{4}}$ . The values of  $M$  and the  $N$  needed in are rather small to achieve the required accuracy. For example, if  $\epsilon = 10^{-7}$  and  $\delta = 5 \times 10^{-5}$ , we need  $M = N = O(10^3)$ .

We use (6.8) with  $\alpha = \beta = c = 1$  for numerical computation. Choose  $\epsilon = 10^{-7}$  and  $M = N = 200$ . We list in Table 4 the pointwise values of the solutions and derivatives along  $y = 2\pi - \epsilon$ , and illustrate in Figure 5 the profile of solutions. The convergence of the solutions (6.8) for this model is also fast for  $\epsilon = 0.1 - 10^{-7}$ , as indicated by Theorem 6.1.

## 7 Collocation Trefftz Method

In this section we consider a boundary-type of numerical method, called the collocation Trefftz method [7, 8, 9] for the singularly perturbed problem. The main idea of the method is to use particular solutions as the admissible functions which satisfy the partial differential equation, so that the numerical efforts will be paid to approximate the boundary conditions. We then force the residuals to be zero at some collocation points on the boundary. The optimal convergence rates for such a method can be achieved.

To demonstrate this technique, we take Model *II* as an example, and express its solution in the form

$$v = \sum_{k=1}^m \left\{ \tilde{a}_k \phi_k(x, y) + \tilde{b}_k \psi_k(x, y) + \tilde{a}_k^* \phi_k^*(x, y) + \tilde{b}_k^* \psi_k^*(x, y) \right\}, \quad (7.1)$$

where the basis functions  $\phi_k(x, y)$ ,  $\psi_k(x, y)$ ,  $\phi_k^*(x, y)$  and  $\psi_k^*(x, y)$  are given in (5.3). The coefficients  $\tilde{a}_k$ ,  $\tilde{b}_k$ ,  $\tilde{a}_k^*$  and  $\tilde{b}_k^*$  are yet to be determined.

Let  $V_m$  be the finite dimensional space of the admissible function  $v$  in (7.1). The collocation Trefftz method is to seek  $u_m = u_m(\tilde{a}_k, \tilde{b}_k, \tilde{a}_k^*, \tilde{b}_k^*) \in V_m$  such that

$$\hat{I}(u_m) = \min_{v \in V_m} \hat{I}(v), \quad (7.2)$$

where

$$\hat{I}(v) = \int_{\Gamma_1} (v - g_1)^2 + \int_{\Gamma_2} (v - g_2)^2 + \int_{\Gamma_3} (v - g_3)^2 + \int_{\Gamma_4} (v - g_4)^2.$$

Here  $\Gamma_i (i = 1, 2, 3, 4)$  denote the boundary segments of domain  $S$ , and the functions  $g_i (i = 1, 2, 3, 4)$  denote the boundary conditions given in (5.1). Define a B-norm as

$$\begin{aligned} \|u - v\|_B &= \sqrt{\hat{I}(v)} \\ &= \left\{ \int_{\Gamma_1} (v - g_1)^2 + \int_{\Gamma_2} (v - g_2)^2 + \int_{\Gamma_3} (v - g_3)^2 + \int_{\Gamma_4} (v - g_4)^2 \right\}^{\frac{1}{2}}. \end{aligned} \quad (7.3)$$

The collocation Trefftz method can also be regarded as a certain kind of the least squares method involving specific quadrature rules. For the approximation of integrals in (7.2), we may choose the Newton-Cotes quadrature formulas. The minimization of  $\hat{I}(v)$  leads to a linear system, and the details of the algorithms for the method can be found in [7, 9]. In fact, we may also handle the models involving the Neumann and the Robin boundary conditions well by the same technique.

We divide each boundary segment  $\Gamma_i (i = 1, 2, 3, 4)$  into  $N_c$  equal subintervals. Each boundary segment contains  $N_c$  collocation points from which the Newton-Cotes quadrature points are chosen. Theoretically, the total number of collocation points is chosen to be larger than that of the unknown coefficients, i.e.,  $4N_c \geq 4m$ . Consequently, we obtain an overdetermined system which can be solved by the QR decomposition, singular value decomposition or the least squares method. Numerical results have been obtained using Mathematica with long working digits for the problems with  $m = 15$  and  $N_c = 25$ . The exact coefficients have also been calculated using (5.4). The computed coefficients and their errors for  $p = 1$  and various values of  $\epsilon$  are listed in Table 5. We see from the table that the relative errors of the leading coefficients are very small.

Furthermore, we consider the changes of the relative errors and the B-norms with respect to  $N_c$  and  $m$ . The computed results are listed in Tables 6 and 7 respectively. We see from Table 6 that the number of collocation points,  $N_c$ , has very minor effect on the accuracy, as long as  $N_c \geq 25$ . From Table 7, we have calculated the asymptotic relation between the B-norm and  $m$  as

$$\|u - v\|_B = O((0.0013)^m). \quad (7.4)$$

Eq. (7.4) displays an exponential convergence rate for the collocation Trefftz method, in which the computed error decays rapidly as  $m$  grows. The computed convergence rates for the first four coefficients of  $a_k (k = 1, 2, 3, 4)$  are given by

$$\begin{aligned} \left| \frac{a_1 - \tilde{a}_1}{a_1} \right| &= O((0.25)^m), & \left| \frac{a_2 - \tilde{a}_2}{a_2} \right| &= O((0.26)^m), \\ \left| \frac{a_3 - \tilde{a}_3}{a_3} \right| &= O((0.27)^m), & \left| \frac{a_4 - \tilde{a}_4}{a_4} \right| &= O((0.29)^m), \end{aligned}$$

respectively.

Note that we may also divide a solution domain into two disjoint or overlapped subdomains, and then choose a combined or the Schwarz iterative method to solve the problem. The collocation Trefftz method can be used in the subdomain with layers or singularities, while other methods, such as standard finite difference or finite element method can be used in the subdomain where the solution is smooth. The relevant research results will be reported elsewhere.

## 8 Concluding remarks

Motivations of this study and relevant works [5, 6] are to derive particular solutions of singularly perturbed PDEs with constant coefficients in rectangular domains which are crucial to the Trefftz method. In Section 2, the particular solutions of (2.1) have been found by the technique of the separation of variables. From the given particular solutions, we have designed deliberately three computational models. These three models can be used as benchmarks of boundary layer problems for testing any numerical methods. Let us give a few remarks about these models.

1. The model of waterfall solutions, called Model *I*, was first given in [5]. The drawback of the Model *I* is its slow convergence rates, and in practice,  $\epsilon$  for Model *I* can only be chosen such that  $\epsilon \geq 10^{-2}$ . In [6] a modified method, called Model *I<sub>M</sub>*, of fast convergence is proposed. While [5] and [6] focus on convergence analysis, this paper is concentrated on the computational aspects for Model *I<sub>M</sub>*. We have shown numerically that for small values of  $\epsilon$ , the convergence of the approximate solution obtained by truncating the exact series solution is of very high order. Surprisingly, when  $\epsilon = 10^{-7}$ , the number of terms  $N$  in the truncated series can even be chosen to be  $N = 0$  for Model *I<sub>M</sub>* with  $\alpha = \beta = c = 1$ . When  $\epsilon = 0.1$ ,  $N = O(10^2)$  is sufficient for Model *I<sub>M</sub>*. Numerical results and profiles of solutions supporting these conclusions have been provided in Tables 1-2 and Figures 1-3, respectively.
2. When  $\alpha = c = 1$  and  $\beta = 0$  in Model *I<sub>M</sub>*, there exist two different boundary layers, one regular and the other parabolic, as discussed in Section 4.3. For this case, we have defined the width of both boundary layers and provided the simplified formulas to evaluate them numerically.
3. For Model *II*, while the solutions with two spikes were proposed and analyzed in [5], we have considered, in this paper, the solutions with four spikes. Model *II* converges rapidly due to the number of terms  $N = 10 - 15$  is sufficient for  $\epsilon = 10^{-1} - 10^{-7}$ . Numerical results demonstrating these are given in Table 3 and Figure 4.
4. In this paper, we have also developed a new model of the non-homogeneous equations, called Model *III*. New error analysis is given in Theorem 6.1 which shows that the fast convergence of Model *III*. Supporting numerical results are given in Table 4 in Figure 5.

Apart from the above points, we have also extend the models to the case with anisotropic diffusion coefficients, as given in Section 3.1. The collocation Trefftz method has also been proposed using the particular solutions obtained in the paper. Numerical experiments on the Trefftz method have been performed using one of the particular solutions.

## References

- [1] M. Abramowitz and I. Stegun, **Handbook of Mathematical Functions with Formulas, Graphs and Mathematical Tables**, Devor Publications, Inc, New York, p. 257, 1970.
- [2] S. Gradshteyn and I. M. Ryzhik, **Table of Integrals, Series, and Products, Corrected and Enlarged Edition**, p. 41, Academic Press, New York, 1980.
- [3] G. Grunberg, *A new method of solution of certain boundary problems for equations of mathematical physics permitting of reparation of variables*, J. Phys., Vol. 10, pp. 301-320, 1946.
- [4] Z. C. Li, **Combined Methods for Elliptic Equations with Singularities, Interfaces and Infinities**, Kluwer Academic Publishers, Boston, London, 1998.
- [5] Z. C. Li, H. Y. Hu, C. H. Hsu and S. Wang, *Particular solutions of singularly perturbed partial differential equations with constant coefficients in rectangular domains, Part I. Convergence Analysis*, Journal of Computational and Applied Mathematics, Vol. 166, No. 1, pp. 181-208, 2004.
- [6] Z. C. Li, H. S. Tasi, S. Wang and J. J. H. Miller, *New models of singularly perturbed differential equations with waterfalls solutions*, Technical report, Department of Applied Mathematics, National Sun Yet-sen University, 2004.
- [7] Z. C. Li, T. T. Lu and H. Y. Hu, *Collocation Trefftz methods for biharmonic equations with crack singularities*, Engineering Analysis with Boundary Elements, Vol. 28, No. 1, pp. 79-96, 2004.
- [8] Z. C. Li, T. T. Lu, H. Y. Hu and A. H.-D. Cheng, *Partical solutions of Laplace's equations on polygons and new models involving mild singularities*, Engineering Analysis with Boundary Elements, Vol. 29, No. 1, pp. 59-75, 2004.
- [9] T. T. Lu, H. Y. Hu and Z. C. Li, *Highly accurate solutions of Motz's problem and the cracked beam problem*, Engineering Analysis with Boundary Elements, Vol. 28, No. 11, pp. 1387-1403, 2004.
- [10] J. J. H. Miller, E. O'Roordan and G. I. Shiskin, **Fitted Numerical Methods for Singular Perturbation Problems**, World Scientific, Singapore, 1996.
- [11] H. G. Roos, M. Stynes, and L. Tobiska, **Numerical Methods for Singularly Perturbed Differential Equations, Convection-Diffusion and Flow Problems**, Springer, 1996.

- [12] S. Wang and Z. C. Li, *A nonconforming combination of the finite element and volume methods with an anisotropic mesh refinement for a singularly perturbed convection-diffusion equation*, Mathematics of Computation, Vol. 72, No. 244, pp. 1689-1709, 2003.

**Table 1.**

The computed solution values along  $y = \pi - \epsilon$  of Model  $I_M$  with  $\alpha = \beta = c = 1$  and  $\epsilon = 10^{-7}$ .

$x$	$\pi - 11\epsilon$	$\pi - 10\epsilon$	$\pi - 9\epsilon$	$\pi - 8\epsilon$	$\pi - 7\epsilon$	$\pi - 6\epsilon$
$u$	3.6789(-1)	3.6791(-1)	3.6796(-1)	3.6809(-1)	3.6846(-1)	3.6945(-1)
$u_x$	1.0557(2)	2.8698(2)	7.8010(2)	2.1205(3)	5.7642(3)	1.5669(4)
$u_y$	3.6787(6)	3.6786(6)	3.6783(6)	3.6776(6)	3.6754(6)	3.6697(6)

$x$	$\pi - 5\epsilon$	$\pi - 4\epsilon$	$\pi - 3\epsilon$	$\pi - 2\epsilon$	$\pi - \epsilon$	$\pi$
$u$	3.7214(-1)	3.7946(-1)	3.9935(-1)	4.5343(-1)	6.0042(-1)	1.0000
$u_x$	4.2592(4)	1.1578(5)	3.1471(5)	8.5548(5)	2.3254(6)	6.3212(6)
$u_y$	3.6540(6)	3.6114(6)	3.4956(6)	3.1809(6)	2.3254(6)	5.7802(-3)

**Table 2.**

The computed solution values along  $y = \pi - \sqrt{\epsilon}$  for Model  $I_M$  with  $\alpha = c = 1$ ,  $\beta = 0$  and  $\epsilon = 10^{-7}$ .

$x$	$\pi - 11\sqrt{\epsilon}$	$\pi - 10\sqrt{\epsilon}$	$\pi - 9\sqrt{\epsilon}$	$\pi - 8\sqrt{\epsilon}$	$\pi - 7\sqrt{\epsilon}$	$\pi - 6\sqrt{\epsilon}$
$u$	3.6788(-1)	3.6788(-1)	3.6788(-1)	3.6788(-1)	3.6788(-1)	3.6788(-1)
$u_x$	0.0000	0.0000	0.0000	0.0000	0.0000	0.0000
$u_y$	1.1633(3)	1.1633(3)	1.1633(3)	1.1633(3)	1.1633(3)	1.1633(3)

$x$	$\pi - 5\sqrt{\epsilon}$	$\pi - 4\sqrt{\epsilon}$	$\pi - 3\sqrt{\epsilon}$	$\pi - 2\sqrt{\epsilon}$	$\pi - \sqrt{\epsilon}$	$\pi$
$u$	3.6788(-1)	3.6788(-1)	3.6788(-1)	3.6788(-1)	3.6788(-1)	1.0000
$u_x$	0.0000	0.0000	0.0000	0.0000	0.0000	5.0693(6) *
$u_y$	1.1633(3)	1.1633(3)	1.1633(3)	1.633(3)	1.1633(3)	6.0802(-1) *

In the Table,  $N \approx O(10^4)$  for the data denoted by \*, and  $N = 1$  for others.

**Table 3.**

The computed solution values of near boundary along  $y = \pi - \epsilon$  for Model *II* with  $\epsilon = 10^{-7}$ .

$x$	0	$\epsilon$	$2\epsilon$	$3\epsilon$	$4\epsilon$	$5\epsilon$
$u$	8.2436(-1)	6.7015(-1)	5.4478(-1)	4.4287(-1)	3.6002(-1)	2.9267(-1)
$u_x$	-1.7073(6)	-1.3879(6)	-1.1282(6)	-9.1722(5)	-7.4562(5)	-6.0615(5)
$u_y$	-4.1218(6)	-3.3507(6)	-2.7239(6)	-2.2143(6)	-1.8001(6)	-1.4633(6)

$x$	$\pi - 5\epsilon$	$\pi - 4\epsilon$	$\pi - 3\epsilon$	$\pi - 2\epsilon$	$\pi - \epsilon$	$\pi$
$u$	1.6879(-1)	2.2663(-1)	2.9413(-1)	3.7279(-1)	4.9306(-1)	8.2436(-1)
$u_x$	5.2427(5)	6.2969(5)	7.1963(5)	8.8998(5)	1.7432(6)	5.8862(6)
$u_y$	2.0038(6)	2.6231(6)	3.1741(6)	3.2413(6)	1.7432(6)	-4.1218(6)

**Table 4.**

The computed solution values near boundary along  $y = 2\pi - \epsilon$  for Model *III* with  $\epsilon = 10^{-7}$ .

$x$	$2\pi - 11\epsilon$	$2\pi - 10\epsilon$	$2\pi - 9\epsilon$	$2\pi - 8\epsilon$	$2\pi - 7\epsilon$	$2\pi - 6\epsilon$
$u$	5.0368(-2)	7.5493(-2)	1.1202(-1)	1.6417(-1)	2.3683(-1)	3.3469(-1)
$u_x$	2.0605(5)	3.0197(5)	4.3563(5)	6.1563(5)	8.4584(5)	1.1156(6)
$u_y$	-2.5184(5)	-3.7746(5)	-5.6010(5)	-8.2085(5)	-1.1841(6)	-1.6734(6)

$x$	$2\pi - 5\epsilon$	$2\pi - 4\epsilon$	$2\pi - 3\epsilon$	$2\pi - 2\epsilon$	$2\pi - \epsilon$	$2\pi$
$u$	4.5984(-1)	6.0653(-1)	7.5000(-1)	8.2436(-1)	6.7957(-1)	0.0000
$u_x$	1.3795(6)	1.5163(6)	1.2500(6)	7.4453(-8)	-3.3978(6)	-1.1204(7)
$u_y$	-2.2992(6)	-3.0326(6)	-3.7500(6)	-4.1218(6)	-3.3978(6)	0.0000

**Table 5.**

The approximate coefficients and their relative errors for Model *II* with  $m = 15$  and  $N_c = 25$ .

$\epsilon$	$\tilde{a}_1$	$\tilde{a}_2$	$\tilde{a}_3$	$\tilde{a}_4$
$10^{-1}$	36.9452	18.4726	6.1575	1.5393
$10^{-2}$	369.4528	184.7264	61.5754	15.3938
$10^{-3}$	3694.5280	1847.2640	615.7546	153.9386
$10^{-4}$	36945.2804	18472.6401	6157.5466	1539.3865

$\epsilon$	$\frac{\tilde{a}_1 - a_1}{a_1}$	$\frac{\tilde{a}_2 - a_2}{a_2}$	$\frac{\tilde{a}_3 - a_3}{a_3}$	$\frac{\tilde{a}_4 - a_4}{a_4}$
$10^{-1}$	6.30(-13)	2.52(-12)	1.13(-11)	5.98(-11)
$10^{-2}$	1.51(-9)	5.40(-9)	2.02(-8)	8.32(-8)
$10^{-3}$	1.82(-9)	6.50(-9)	2.42(-8)	9.87(-8)
$10^{-4}$	1.82(-9)	6.50(-9)	2.42(-8)	9.87(-8)

**Table 6.**

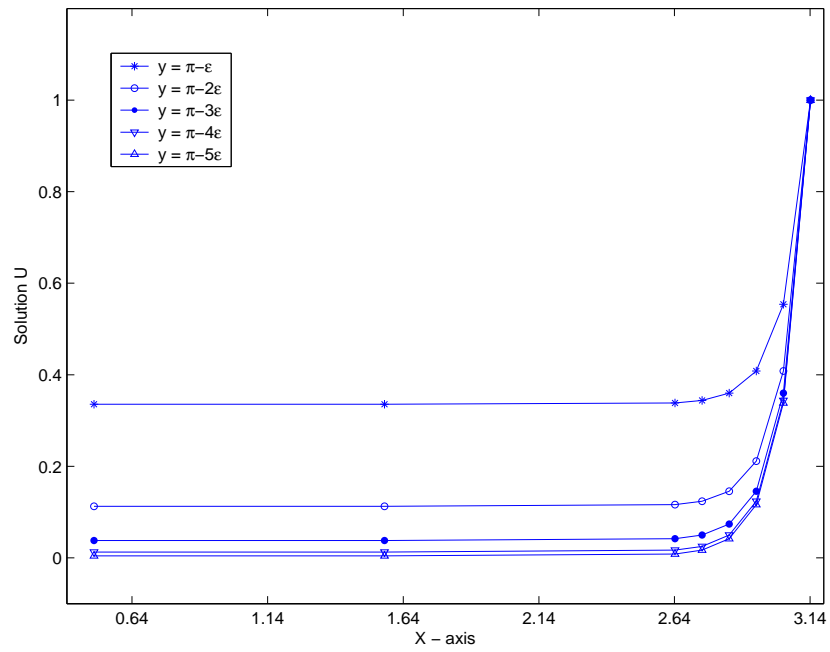
The relative errors and B-norms for Model *II* with  $\epsilon = 10^{-2}$  when  $m = 15$ .

$N_c$	$\frac{\tilde{a}_1 - a_1}{a_1}$	$\frac{\tilde{a}_2 - a_2}{a_2}$	$\frac{\tilde{a}_3 - a_3}{a_3}$	$\frac{\tilde{a}_4 - a_4}{a_4}$	$\ u - v\ _B$
25	4.56(-8)	1.60 (-7)	5.80(-7)	2.27(-6)	1.21(-49)
30	1.09(-8)	3.81(-8)	1.37(-7)	5.30(-7)	1.64(-47)
35	2.88(-8)	9.95 (-8)	3.50(-7)	1.32(-6)	7.58(-44)
40	5.20(-8)	1.78 (-7)	6.19(-7)	2.29(-6)	2.04(-41)

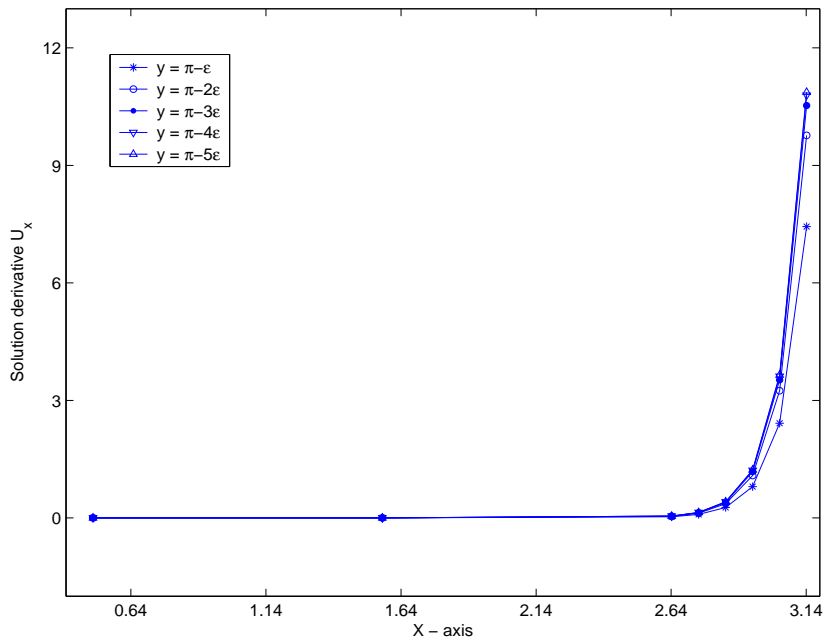
**Table 7.**

The relative errors and B-norms for Model *II* with  $\epsilon = 10^{-2}$  when  $N_c = 25$ .

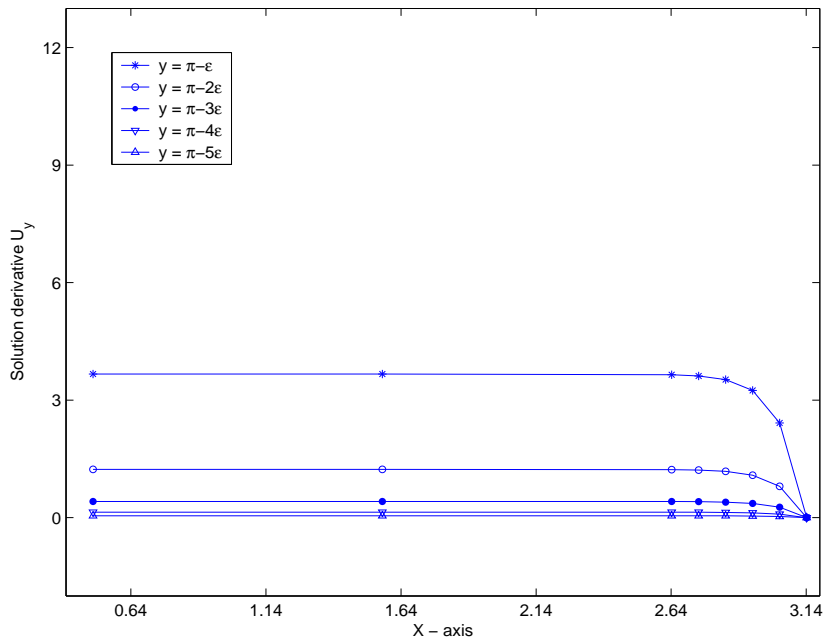
$m$	$\frac{\tilde{a}_1 - a_1}{a_1}$	$\frac{\tilde{a}_2 - a_2}{a_2}$	$\frac{\tilde{a}_3 - a_3}{a_3}$	$\frac{\tilde{a}_4 - a_4}{a_4}$	$\ u - v\ _B$
5	4.42(-2)	1.17(-1)	2.62(-1)	5.11(-1)	7.11(-21)
7	5.45(-3)	1.60(-2)	4.26(-2)	1.07(-1)	2.27(-27)
9	3.75(-4)	1.18(-3)	3.55(-3)	1.06(-2)	9.34(-34)
11	1.36(-5)	4.52(-5)	1.48(-4)	5.04(-4)	3.81(-40)
13	2.40(-7)	8.29 (-7)	2.92(-6)	1.10(-5)	1.23(-46)
15	4.56(-8)	1.60 (-7)	5.80(-7)	2.27(-6)	1.21(-49)



(a) The computed solution along various segments near the layer  $y = \pi$  for Model  $I_M$  with  $\alpha = \beta = c = 1$  and  $\epsilon = 0.1$ .



(b) The curves of derivatives  $u_x$  near the layer  $y = \pi$  for Model  $I_M$  with  $\alpha = \beta = c = 1$  and  $\epsilon = 0.1$ .



(c) The curves of derivatives  $u_y$  near the layer  $y = \pi$  for Model  $I_M$  with  $\alpha = \beta = c = 1$  and  $\epsilon = 0.1$ .

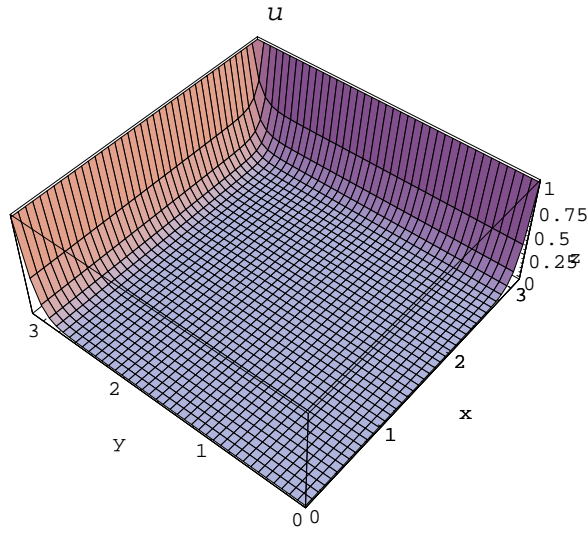


Figure 2: The profile of solution  $u$  on  $[0, \pi]^2$  for Model  $I_M$  with  $\alpha = \beta = c = 1$ , and  $\epsilon = 0.1$ .

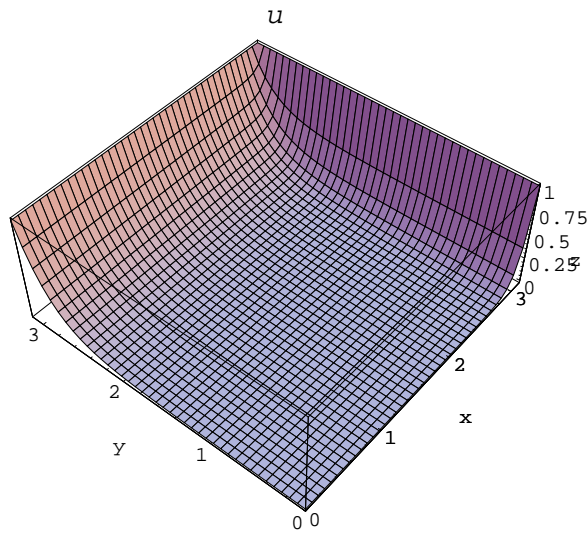


Figure 3: The profile of solution  $u$  on  $[0, \pi]^2$  for Model  $I_M$  with  $\alpha = c = 1, \beta = 0$ , and  $\epsilon = 0.1$ .

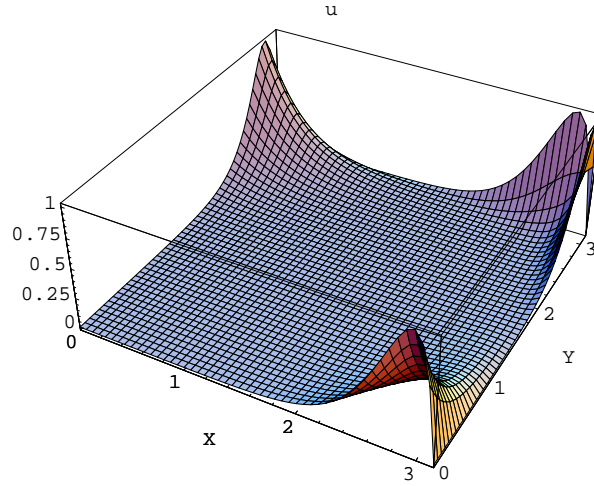


Figure 4: The profile of solution  $u$  on  $[0, \pi]^2$  for Model *II* with  $\epsilon = 0.1$ .

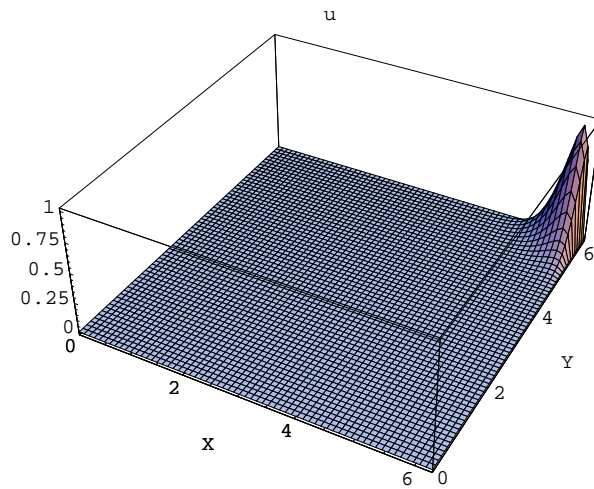


Figure 5: The profile of solution  $u$  on  $[0, 2\pi]^2$  for Model *III* with  $\epsilon = 0.1$ .